Infinite Science
Publishing

Research Article

Concentration Dependent MPI Tracer Performance

Norbert Löwa* · Patricia Radon · Olaf Kosch · Frank Wiekhorst

Physikalisch-Technische Bundesanstalt, Berlin, Germany
*Corresponding author, email: norbert.loewa@ptb.de

Abstract

Magnetic Particle Imaging (MPI) and Magnetic Particle Spectroscopy (MPS) usually require a reference sample measurement to provide information about the non-linear dynamic magnetic behavior of a specific magnetic nanoparticle (MNP) type. This reference sample based approach presupposes that this dynamic magnetization behavior of MNP is concentration independent. We investigated Resovist® and its precursor Ferucarbotran at different concentrations to verify this assumption by means of MPS. Remarkably, for Resovist® we found a strong concentration dependence of the MPS signal. Above an iron concentration of about 150 mmol/L the shape of the moment and phase spectra changed with increasing iron concentration. In contrast, for Ferucarbotran we found no concentration dependence of the dynamic magnetic behavior even though at a two-fold higher initial concentration. Our experimental results indicate that the dynamic magnetic behavior of MPI tracers may be altered at higher concentrations and should be studied prior to MPI by MPS experiments.

I. Introduction

Magnetic Particle Imaging (MPI) is a promising method capable for quantitative visualization of magnetic nanoparticles (MNP) exploiting their nonlinear dynamic magnetization curve. Obtaining the spatial MNP distribution from measured MPI signals generally requires image reconstruction. Therefore, the expected signal of a point-like source at every possible position in the scanner has to be known. Since an exact analytical model of the nonlinear dynamic magnetization behavior of MNP is still not available existing MPI systems use a voxel-sized reference sample to acquire the so called system function. To ensure high spatial resolution at best signal-to-noise-ratio (SNR) the small sample volume is usually measured at highest MNP concentration [1, 2].

Magnetic Particle Spectroscopy (MPS) is based on the same physical principle as MPI waiving of any spatial encoding and has been proven a straightforward technique to study the MPI performance of MNP. Furthermore, MPS is ideally suitable to quantify MNP in different environments (e.g. cells, blood, tissue) down to the nanogram range [3–5]. Quantification is achieved by comparison of MPS signals of the sample with a reference of known MNP content.

However, all reference sample based approaches presume that the dynamic magnetization behavior of MNP does not change, e.g. caused by viscosity changes [6], aggregation [3] or concentration dependent dipole-dipole interactions [7].

Here, we searched for concentration dependent MPS signal changes of the two MNP systems Resovist® (RES) and its precursor Ferucarbotran (FER), both stabilized by a carboxydextran shell. FER (Meito Sangyo, Japan) is the magnetically active constituent of RES (Bayer Health-Care, Germany). The precursor FER is then formulated (i.a. by adjustment of osmolality and pH value) by Bayer (formerly Schering AG) yielding the MRI liver contrast

agent RES. Note, that the FER sample investigated here was not the direct precursor of RES used in this study. Both MNP types have been thoroughly investigated for their magnetic properties [4, 7–9] and were intensively studied in the field of MPI [1, 2] over the last years. Recently, it has been reported that both RES and FER exhibit a bimodal size distribution arising from primary particles and their stable aggregates (i.e. clusters of primary particles) [8, 9].

II. Material and Methods

II.I. Samples

The iron molar concentration of RES and FER was determined using phenanthroline spectrophotometric iron quantification assay after dissolution of the samples in hydrochloric acid. The resulting initial iron concentrations of RES and FER were 470 mmol/L and 940 mmol/L, respectively.

We used filtered ultra-pure water to dilute series of RES and FER samples down to ratios of 1:1.2, 1:1.3, 1:1.5, 1:1.7, 1:1.8, 1:2, 1:3, 1:4, 1:5, 1:6, 1:7, 1:8, 1:9, and 1:10. For MPS measurements 30 μL of liquid sample volume were filled in PCR tubes (fast reaction tube with cap, Appl. Biosystems, USA). In addition to liquid samples, 15 μL of the initial samples of highest concentration were immobilized by freeze-drying after adding 15 μL mannitol solution (5% w/v) to maintain a uniform distribution of MNP during freeze drying. For DLS measurements the iron concentration was adjusted to 1.25 mmol/L. M(H) measurements were performed using polycarbonate capsules filled with 70 μL of liquid sample volume (1:10 dilution).

II.II. Particle size analysis

To determine the effective magnetic domain size, i.e. the size of the magnetically active part of the MNP cores, we measured the quasistatic magnetization M(H) at room temperature as a function of applied field strength (up to 5 T) of the samples by means of a commercial DC-susceptometer (MPMS XL, Quantum Design, USA). Magnetic size distributions were extracted from fitting the magnetization data M(H) using the Langevin model with a bimodal log-normal distribution of spherical non-interacting MNP, as done before for RES and FER [9, 10]. Furthermore, the MNP samples were measured by dynamic light scattering (DLS) (Zetasizer NanoZS, Malvern, UK) to determine the volume weighted hydrodynamic size distributions. The deconvolution of the resulting autocorrelation function was accomplished using a non-negatively constrained least square fitting algorithm.

II.III. Magnetic Particle Spectroscopy

To measure the spectral nonlinear magnetic response of the samples exposed to a time varying magnetic excitation field we used a magnetic particle spectrometer (Bruker Biospin, GER) operating at a fixed frequency $f_{excite} = 25$ kHz. For the MPS measurement, MNP-filled PCR tubes were placed in the spectrometers transmit coil and a strong excitation field ($B_{excite} = 5$ mT up to 25 mT) was applied. The induced magnetization of the MNP was recorded for 1 s by the receiving coils. By Fourier transformation of the temporal response signal the spectral components with distinctive moments μ_k and phases ϕ_k at odd multiples k of f_{excite} are obtained. For simplicity, even harmonic components have not been considered.

III. Results

III.I. Particle size analysis

Fig. 1 shows the effective magnetic core and hydrodynamic size distribution extracted from DC-susceptomery and DLS measurements, respectively. Apparently, there are only little differences between RES and FER. More particularly, the hydrodynamic size of RES is about 10 nm larger compared to FER, whereas the medians of the effective magnetic size distribution did not change significantly. The main difference between the magnetic size distributions is the broader distribution width σ (logarithm of the geometric standard deviation) of the small population of RES compared to FER with $\sigma = 0.34(1)$ and $\sigma = 0.49(2)$, respectively.
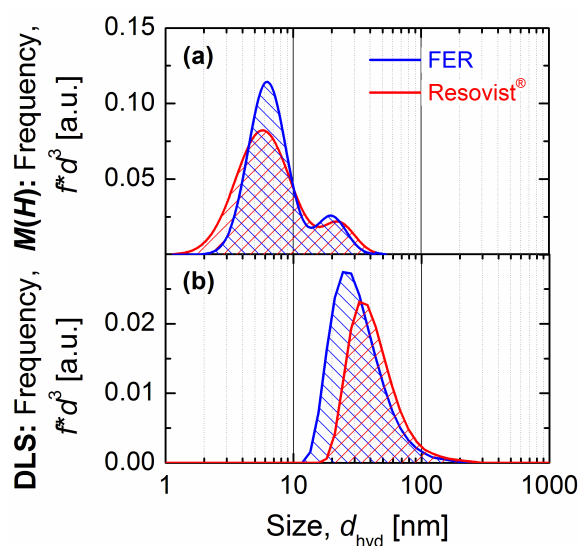

Figure 1: (a) Volume weighted size distributions of FER (blue) and RES as determined by DC-susceptometry (effective magnetic core size) and (b) DLS (hydrodynamic size) measurement.

III.II. Concentration-dependent Magnetic Particle Spectroscopy

MPS measurements of liquid FER and RES samples at different iron concentrations were performed to study the concentration dependency of the odd harmonic magnetic moment μ_k and phase spectrum ϕ_k. The odd harmonic magnetic moment spectra μ_k of RES and FER presented in Fig. 2 (upper graphs) were normalized to the respective iron amount. Spectra of RES and FER are almost identical at highest dilution (1:10, blue lines). Whereas, the corresponding phase spectrum (Fig. 2, lower graphs) of RES exhibits a pronounced minimum at about $k = 11$ which was not observed for FER.
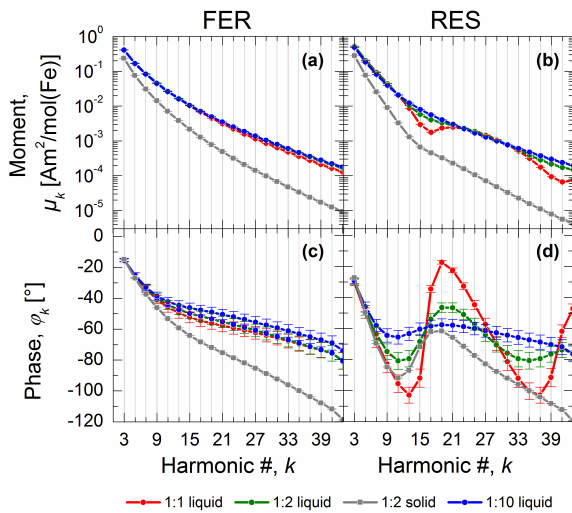

Figure 2: Odd harmonics of the MPS magnetic moment μ_k (a), (b) and phase spectra ϕ_k (c), (d). MPS measurements ($B_{\text{excite}} = 25$ mT, $f_{\text{excite}} = 25$ kHz) were performed on FER and RES with different dilution levels in liquid (1:1, 1:2, 1:10) and solid (1:2) state. To guide the eyes the datapoints of each spectrum μ_k are connected by a line. The uncertainty bars indicate the intrinsic noise of the spectrometer and the sample container variance ($n = 10$).

Moreover, for higher concentrated FER the shape of the magnetic moment and phase spectra does not change significantly. In contrast, the MPS spectra of RES show a distinct concentration dependency characterized by attenuation and amplification of certain harmonics in the phase and magnetic moment spectrum with increasing iron concentration. Interestingly, the minima and maxima of the magnetic moment spectra are correlated with the inflection points of the wave-like phase spectrum, which is clearly seen for the initial concentration of RES. After immobilization of the sample the complete magnetic moment spectrum of FER is strongly reduced in amplitude and an increased signal decay of higher harmonics is observed. For immobilized RES the same trend of an overall signal reduction is visible; however, it still exhibits the wave-like shape clearly visible

in the phase spectrum. Thus, the observed MPS signal deformations at higher concentrations are not caused by chain formation which can be precluded in a solid matrix of the immobilized samples.

To obtain a more detailed analysis of the concentration dependency of the MPS signal of RES a dilution series with subtler concentration step graduation was prepared and analyzed. Fig. 3 shows the most characteristic harmonics of the moment (μ_{17}) and phase spectra (ϕ_{13}, ϕ_{19}) of each dilution step.
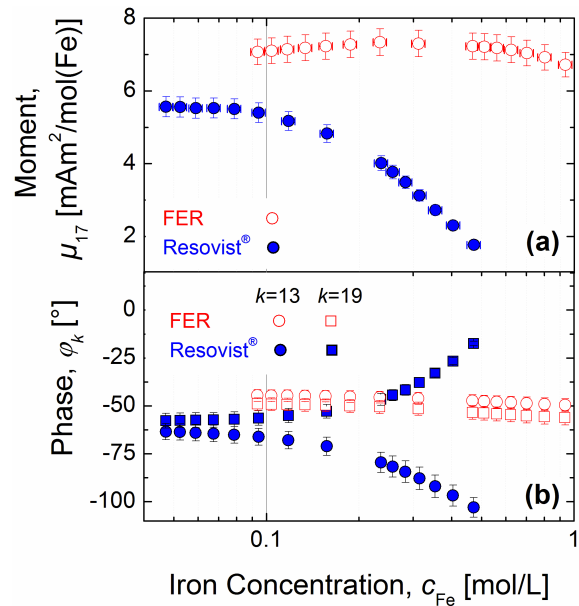

Figure 3: (a) Amplitude of the 17th harmonic in dependence of iron concentration. (b) Phase signal of the 13th (circles) and 19th harmonic (squares) in dependence of iron concentration. All MPS signals were measured at $B_{\text{excite}} = 25$ mT, $B_{\text{excite}} = 25$ kHz on 30 μL sample volume using dilutions of FER (red symbols) and RES (blue symbols). The uncertainty bars indicate the intrinsic noise of the spectrometer and the sample container variance ($n = 10$).

As can be seen, these spectral components of RES (blue filled symbols) exhibit a concentration dependent profile saturating at concentrations below 100 mmol/L. For comparison, the corresponding moment and phase values of the selected harmonics of FER (open red symbols) are nearly constant over the range of concentrations. For 10 different batches of RES the variance of μ_{17} and ϕ_{19} was 22% and 2% (for FER 6% and 4%), respectively. Furthermore, concentration dependent changes in MPS signals may depend on the applied excitation field B_{excite}, as well. To study this, we determined the pair wise root mean squared deviation (RMSD) of the phase spectrum (from $k = 3$ to $k = 19$) for each sample (1:1 to 1:9) with respect to the lowest concentrated sample (1:10) for different excitation fields ($B_{\text{excite}} = 5$ mT to 25 mT). Fig. 4 shows the B_{excite} and c_{Fe} dependent RMSD values for RES as a color scale map. It emerges

that high iron concentrations (>250 mmol/L) result in strong changes of MPS phases compared to the diluted state showing RMSD values above 4°. The RMSD change increases up to 26° for highest B_{excite}. Below an iron concentration of about 150 mmol/L the RMSD is smaller than 1° for all excitation fields applied here which is highlighted by a red line in Fig. 4.
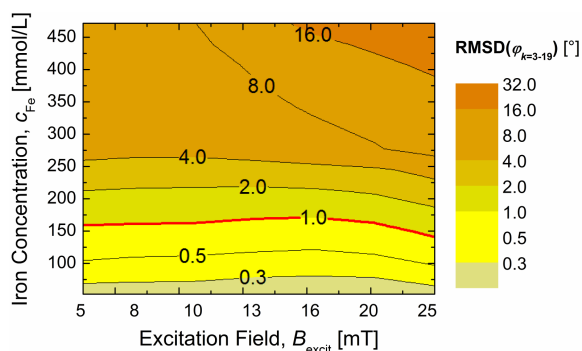

Figure 4: Color map of MPS-phase changes of RES as a function of iron concentration c_{Fe} compared to the sample of highest dilution for various excitation fields B_{excite} (5 mT up to 25 mT). Changes are represented by the sum of pair wise root mean squared deviations (RMSD) of ϕ_k ($k = 3, 5, \ldots, 19$) calculated for each RES concentration (1:1 to 1:9) and B_{excite}. Below an iron concentration of about 150 mmol/L the RMSD is less than 1° (marked by a red line).

IV. Discussion

We have shown that RES and its magnetically active ingredient FER are only slightly different according to size and magnetic properties in higher dilutions as measured by DLS and DC-susceptometry, respectively. The similarity was also found for MPS signals of diluted RES and FER. Below 100 mmol/L no significant differences in the moment spectrum and small differences in the phase spectrum could be observed. Remarkably, RES shows an unexpectedly strong concentration dependence of the MPS signal. Above an iron concentration of about 150 mmol/L both, the moment and phase spectra, exhibit a wave-like shape developing with increasing iron concentration. Given that MNP chain formation could be excluded this effect can be attributed to magnetic dipole-dipole interactions between individual MNP at high concentrations, as has already been reported before [7]. Interestingly, this effect is not present in FER even at a two-fold higher concentration. It still remains unclear if the concentration dependent changes in MPS signals result from the formulation of RES or whether it is an effect of aging. Nevertheless, we observed this for different batches of RES but for no batch of FER.

V. Conclusion

Our experimental results indicate that the dynamic magnetic behaviour of an MPI tracer may be concentration dependent and should be studied prior to MPI experiments. Particularly, for MPI experiments using RES it may be necessary to record a system function using a reference sample at an iron concentration below 150 mmol/L to guarantee a valid image reconstruction of a sample having much lower MNP concentrations. Moreover, a system function acquired with highly concentrated RES may be only valid for the image reconstruction of a small range of tracer concentrations. In contrast, for FER we found no concentration dependence of the dynamic magnetic behavior even though a two-fold higher initial concentration was used. FER should thus be preferred for phantom experiments where full in vivo compatibility is not mandatory. MPI experiments investigating the concentration dependence of MNP under 3D excitation are important to validate the relevance of our spectroscopic measurement results.

Acknowledgments

References

[1] J. Rahmer, A. Halkola, B. Gleich, I. Schmale, and J. Borgert. First experimental evidence of the feasibility of multi-color magnetic particle imaging. *Phys. Med. Biol.*, 60(5):1775, 2015. doi:10.1088/0031-9155/60/5/1775.

[2] M. G. Kaul, O. Weber, U. Heinen, A. Reitmeier, T. Mummert, C. Jung, N. Raabe, T. Knopp, H. Ittrich, and G. Adam. Combined preclinical magnetic particle imaging and magnetic resonance imaging: Initial results in mice. *Fortschr. Röntgenstr.*, 187(05):347–352, 2015. doi:10.1055/s-0034-1399344.

[3] W. C. Poller, N. Löwa, F. Wiekhorst, M. Taupitz, S. Wagner, K. Möller, G. Baumann, V. Stangl, L. Trahms, and A. Ludwig. Magnetic particle spectroscopy reveals dynamic changes in the magnetic behavior of very small superparamagnetic iron oxide nanoparticles during cellular uptake and enables determination of cell-labeling efficacy. *J. Biomed. Nanotech.*, 12(2):337–346, 2016. doi:10.1166/jbn.2016.2204.

[4] N. Löwa, F. Wiekhorst, I. Gemeinhardt, M. Ebert, J. Schnorr, S. Wagner, and L. Trahms. Cellular uptake of magnetic nanoparticles quantified by magnetic particle spectroscopy. *IEEE Trans. Magn.*, 49(1):275–278, 2013. doi:10.1109/TMAG.2012.2218223.

[5] P. Radon, M. Liebl, N. Pompner, M. Stapf, F. Wiekhorst, K. Gitter, I. Hilger, S. Odenbach, and L. Trahms. Magnetic particle spectroscopy to determine the magnetic drug targeting efficiency of different magnetic nanoparticles in a flow phantom. *IEEE Trans. Magn.*, 51(2):1–4, 2015. doi:10.1109/TMAG.2014.2326889.

[6] T. Wawrzik, T. Yoshida, M. Schilling, and F. Ludwig. Debye-based frequency-domain magnetization model for magnetic particle spectroscopy. *IEEE Trans. Magn.*, 51(2):1–4, 2015. doi:10.1109/TMAG.2014.2332371.

[7] D. Eberbeck and L. Trahms. Experimental investigation of dipolar interaction in suspensions of magnetic nanoparticles. *J. Magn. Magn. Mater.*, 323(10):1228–1232, 2011. doi:10.1016/j.jmmm.2010.11.011.

[8] A. F. Thünemann, S. Rolf, P. Knappe, and S. Weidner. In situ analysis of a bimodal size distribution of superparamagnetic nanoparticles. *Anal. Chem.*, 81(1):296–301, 2009. doi:10.1021/ac802009q.

[9] D. Eberbeck, F. Wiekhorst, S. Wagner, and L. Trahms. How the size distribution of magnetic nanoparticles determines their magnetic particle imaging performance. *Appl. Phys. Lett.*, 98(18):182502, 2011. doi:10.1063/1.3586776.

[10] N. Löwa, D. Eberbeck, U. Steinhoff, F. Wiekhorst, and L. Trahms. Potential of improving mpi performance by magnetic seperation. In *Springer Proceedings in Physics*, volume 140, pages 73–78. Springer, Berlin/Heidelberg, 2012. doi:10.1007/978-3-642-24133-8_12.